molbank

MDPI

Communication

(5-Chloroquinolin-8-yl)-2-fluorobenzoate. The Halogen Bond as a Structure Director

Rodolfo Moreno-Fuquen [1,*], Juan Carlos Castillo [2], Rodrigo Abonía [1], Jaime Portilla [2] and José Antonio Henao [3]

1 Department of Chemistry, Universidad del Valle, A.A. 25360, Santiago de Cali, Colombia; rodrigo.abonia@correounivalle.edu.co
2 Department of Chemistry, Universidad de los Andes, Bogotá 111711, Colombia; jc.castillom@uniandes.edu.co (J.C.C.); jportill@uniandes.edu.co (J.P.)
3 Escuela de Química, Facultad de Ciencias, Universidad Industrial de Santander, Apartado 678, Bucaramanga, Colombia; jahenao@gmail.com
* Correspondence: rodolfo.moreno@correounivalle.edu.co; Tel.: +57-2-339-3248

Academic Editor: René T. Boeré
Received: 16 January 2017; Accepted: 28 February 2017; Published: 9 March 2017

Abstract: Structures containing 8-hydroxyquinoline scaffold are useful for anticancer drug development. The title ester (5-chloroquinolin-8-yl)-2-fluorobenzoate was prepared by the reaction of 2-fluorobenzoyl chloride with 5-chloro-8-hydroxyquinoline. The structure of the title compound was assigned by diverse spectroscopic techniques. Moreover, a crystallographic study was undertaken and its supramolecular characteristics were analyzed. Thus, the central ester fragment C8/O1/C10(O2)/C11 is almost planar with a root mean square (r.m.s.) deviation of 0.0612 Å and it makes dihedral angles of 76.35(6)° and 12.89(11)°, with quinoline and phenyl rings respectively. The structure shows C–H...X (X = halogen) non-classical hydrogen bonds. It also has a halogen . . . halogen distance less than the sum of the van der Waals radii (3.2171(15) Å). As a result of interactions with halogen atoms, chains of centrosymmetric dimer that form edge-fused $R^2_2(18)$ rings run parallel to the plane (100).

Keywords: 8-hydroxyquinoline; antitumor agents; single-crystal X-ray diffraction; supramolecular chemistry

1. Introduction

The *N*-heterocycles such as quinolines are important starting pharmacophores for preparing therapeutic agents with a wide spectrum of biological activities, such as antimalarial [1], antiviral [2], antibacterial [3], anti-inflammatory [4], and mainly antitumor [5–7] activities. The incorporation of diverse halogen atoms into their structures, especially chlorine and fluorine, can lead to important changes in their chemical, pharmacological and physical properties [8–10]. In this sense, and continuing with our current studies on the structural properties of novel aryl and heteroaryl benzoates of synthetic and biological interest [11–15], the fluoroquinoline-derivative **3** was obtained by a direct reaction of 2-fluorobenzoyl chloride **1** and 5-chloro-8-hydroxyquinoline **2** in the presence of triethylamine as base (Scheme 1).

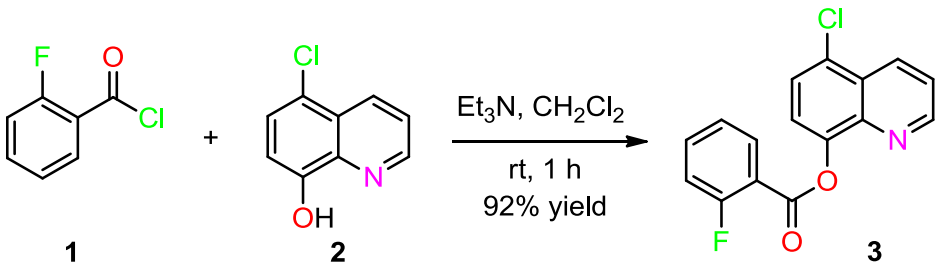

Scheme 1. Synthesis of (5-chloroquinolin-8-yl)-2-fluorobenzoate **3**.

2. Results and Discussion

The title product **3** was obtained in 92% yield from equimolar amounts of 2-fluorobenzoyl chloride **1** and 5-chloro-8-hydroxyquinoline **2** through a nucleophilic acyl substitution reaction as shown in Scheme 1. Reaction proceeded at room temperature in dichloromethane as solvent and triethylamine as base. The starting materials were consumed after 1h of stirring (TLC control) and the residue was purified by column chromatography on silica gel using dichloromethane as eluent, affording a white solid. After analysis by analytical and spectroscopic techniques (i.e., FTIR, 1D NMR and mass spectrum), formation of the new ester **3** was confirmed.

Although compound **3** is a known and apparently commercial molecule [16], no details about its spectroscopic and crystallographic analysis could be found. For that reason, a complete analytical and spectroscopic characterization (i.e., FTIR, 1D NMR, mass and HRMS spectra) was performed in this work, see Material and Methods section.

The most relevant spectroscopic features for compound **3** correspond to the presence of C=O and C–O absorption bands at 1741 and 1213/1066 cm^{-1}, respectively, in the FTIR spectrum. The ^{1}H-NMR spectrum of the quinoline-derivative **3** recorded at 25 °C in $CDCl_3$ shows nine different aromatic protons in the range of 7.22–8.95 ppm and the absence of the phenolic proton signal, which confirms the formation of the ester functionality. The presence of nine aromatic carbon atoms (=CH), six quaternary carbon atoms and the carbonyl group (C=O) at 162.8 ppm in the ^{13}C-NMR spectrum, agrees with the proposed structure for compound **3**. Two molecular ions with m/z 303/301 (complying with the Cl-rule), and a base peak with m/z 123 [M–C_9H_5ClNO] in the mass spectrum, is also consistent with the structure **3**.

2.1. Structural Analysis

Single crystals of compound **3** suitable for X-ray diffraction were grown via slow evaporation in acetone at room temperature. The X-ray diffraction analysis (see Figures 1–3 and Tables 1 and 2), also confirmed the proposed structure for the quinoline-ester **3**.

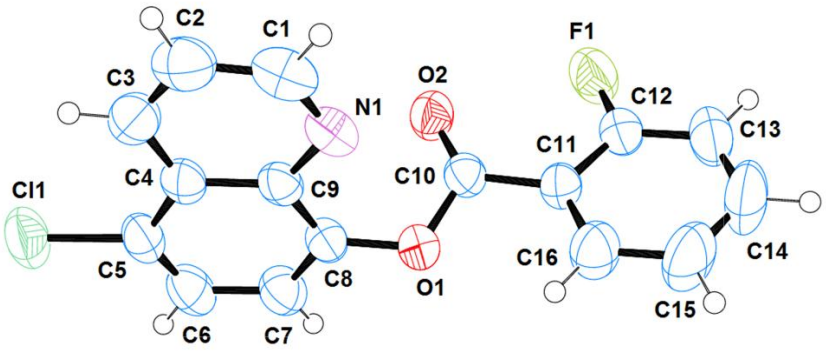

Figure 1. Oak Ridge Thermal Ellipsoid Plot (ORTEP) drawing of the asymmetric unit for compound **3**; ellipsoids are displayed at the 50% probability level.

Table 1. Selected bond lengths [Å], angles [°] and torsion angles [°] for compound **3**.

Bond lengths	
C(5)-Cl(1); 1.7310(19)	O(1)-C(10); 1.355(2)
C(9)-N(1); 1.361(2)	C(10)-O(2); 1.191(2)
C(1)-N(1); 1.300(3)	C(10)-C(11); 1.473(2)
C(8)-O(1); 1.389(2)	C(12)-F(1); 1.337(3)
Angles	
C(8)-O(1)-C(10); 117.06(14)	O(1)-C(10)-C(11); 110.26(15)
Torsion angles	
O(2)-C(10)-C(11)-C(12); −11.7(3)	O(2)-C(10)-C(11)-C(12); −11.7(3)
F(1)-C(12)-C(11)-C(10); −5.5(3)	O(1)-C(10)-C(11)-C(16); −16.1(3)
C(9)-C(8)-O(1)-C(10); −70.6(2)	

Short atomic contacts involving halogen atoms have been used as design devices in crystalline engineering for many years [17]. At the present time, halogen bonds prove their importance, validating their properties in the organization of molecules in the crystalline state. The study, at supramolecular level, of intermolecular interactions in the title compound, showed that the crystal packing has C–H ... X (X-halogen atom) hydrogen short contacts. In addition, in the crystalline structure of the present compound, non-covalent interactions between halogen atoms, analogous to hydrogen bonds, were observed. The halogen bond is an attractive interaction between an electrophilic region (σ-hole) [18] which emerges on the surface of the halogen atom, and it can interact favorably with negative sites on other molecules. The title structure shows a halogen ... halogen interaction, with a Cl1...F1 distance less than the sum of the van der Waals radii (3.2171(15) Å). In the title compound **3**, central fragment C8/O1/C10(O2)/C11 is almost planar with a r.m.s. deviation of 0.0612 Å and it makes dihedral angles of 76.35(6)° and 12.89(11)° between quinoline and phenyl rings, respectively. The carbonyl O2 atom is *syn* positioned with respect to the fluorine atom. Bond lengths and bond angles in crystals of **3** are in a good agreement with those of a similar compound, the 8-quinolyl benzoate [19].

2.2. Supramolecular Features

The packing arrangement of the title compound **3** can be described by hydrogen C–H ... F close contacts and halogen bonded C–Cl ... F intermolecular contacts and they are responsible for crystal growth (See Table 2). In these interactions, the C6–H6 acts as a hydrogen-bond donor to the $F1^{ii}$ atom, forming centrosymmetric dimers and edge-fused $R^2_2(18)$ rings. These rings are linked by halogen C–Cl ... F bonds, which run parallel to (100) (see Figure 2), where the chlorine atom plays the role of halogen bond donor for $F1^{i}$.

Table 2. Non-classical hydrogen and halogen bonding lengths [Å] for compound **3**.

D–H ... A	**D–H**	**H ... A**	**D ... A**	**D–H ... A**
C5–Cl1 ... $F1^{i}$	1.7310(19)	3.2171(15)	4.816(2)	152
C6–H6 ... $F1^{ii}$	0.93	2.57	3.491(3)	169.8
C15–H15 ... $F1^{iii}$	0.93	2.62	3.515(3)	161.5

Symmetry codes: (i) −x + 2, y − 1/2, −z + 3/2; (ii) −x + 1, y − 1/2, −z + 3/2; (ii) −x + 2, −y + 1, −z + 2; (iii) x − 1,y,z.

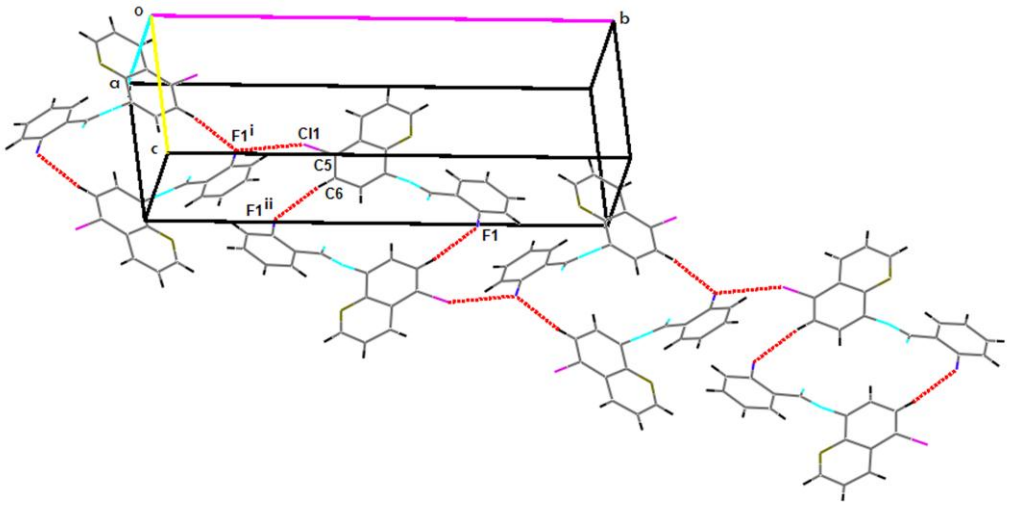

Figure 2. Partial packing diagram showing the two-dimensional sheet network of molecules in the bc plane, the formation of which is governed by the occurrence of C–Cl . . . F halogen bonds and C-H . . . F hydrogen bonds, forming edge-fused $R^2_2(18)$ rings parallel to (100). Hydrogen bonds are depicted with dashed lines. (Symmetry code: (i) −x + 2,y − 1/2,−z + 3/2; (ii) −x + 2,−y + 1,−z + 2).

Interactions on the (100) plane are complemented by other weak hydrogen bonds: The C15–H15 acting as a donor with respect to the F^{iii} atom (see Figure 3 and Table 2). These interactions generate a chain of molecules growing along [001].

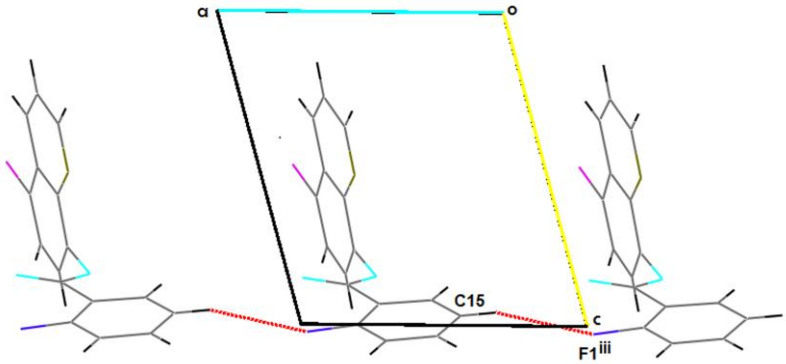

Figure 3. Part of the crystal structure of **3**, showing the formation of C(6) chains along (100). (Symmetry code: (iii) x−1,y,z].

The title structure presents the following geometric shape for the halogen bond, Figure 4.

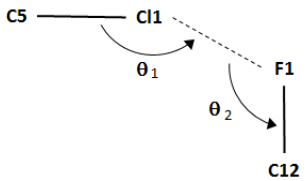

θ1= 152°,

θ2= 111°

Figure 4. Schematic of short halogen interactions for the title compound.

This X . . . X halogen interaction (with $X_1 \neq X_2$) is designated as unsymmetrical contact type II [20]. This interaction has been taken in such a way that the chlorine atom plays the role of the proton at the hydrogen bond. The chlorine atom has been chosen because it is the heavier atom among the halogens

and it is more polarizable and better fulfills the function of expressing an electropositive region on its surface along the halogen bond. This halogen bond punctually proves its importance when its role is validated in the crystalline growth of compound **3**. Halogen bonds become fundamental in the organization of molecules in the crystalline state, much more so when there are no other stronger intermolecular interactions that can direct the growth process.

3. Materials and Methods

3.1. General Information

Melting point was determined on a Büchi melting point B-450 apparatus (Instrumart, South Bulington, VT, USA). IR spectra were recorded on a Shimadzu FTIR 8400 spectrophotometer (Scientific Instruments Inc., Seattle, WA, USA) using KBr disks. NMR spectra were recorded on a Bruker Avance 400 spectrometer (Bruker BioSpin GmbH, Rheinstetten, Germany) operating at 400.13 MHz for ^{1}H and 100.61 MHz for ^{13}C, and using tetramethylsilane as an internal standard. NMR spectroscopic data were recorded in $CDCl_3$ using as internal standards the residual non-deuteriated signal for ^{1}H-NMR and the deuteriated solvent signal for ^{13}C-NMR spectroscopy. Chemical shifts (δ) are in ppm, coupling constants (*J*) are in Hertz (Hz) and the classical abbreviations are used to describe the signal multiplicities. The mass spectrum was obtained on a SHIMADZU-GCMS 2010-DI-2010 spectrometer (Scientific Instruments Inc., Columbia, NC, USA) equipped with a direct inlet probe operating at 70 eV. High resolution mass spectra (HRMS) were recorded on an Agilent Technologies Q-TOF 6520 spectrometer (Agilent Technologies, Waldbronn, Germany) via an electrospray ionization (ESI). Silica gel aluminum plates (Merck 60 F_{254}, Darmstadt, Germany) were used for analytical TLC. The starting fluorobenzoyl chloride **1**, 5-chloro-8-hydroxyquinoline **2**, and triethylamine were purchased from Sigma-Aldrich (San Luis, MO, USA); they were analytical grade reagents, and were used without further purification.

*3.2. Synthesis of (5-Chloroquinolin-8-yl)-2-fluorobenzoate (**3**)*

2-Fluorobenzoyl chloride **1** (119 μL, 1.0 mmol) was added dropwise to a solution of 5-chloro-8-hydroxyquinoline **2** (179 mg, 1.0 mmol) and triethylamine (167 μL, 1.2 mmol) in dichloromethane (5.0 mL). The mixture was stirred at room temperature for 1 h until the starting materials were no longer detected by thin-layer chromatography. After solvent was removed under reduced pressure, water (5.0 mL) was added, and the aqueous solution was extracted with ethyl acetate (2 × 5.0 mL). The combined organic layers were dried with anhydrous magnesium sulfate, and the pure product **3** was obtained as a white solid (277 mg, 92%) after purification by column chromatography on silica gel using dichloromethane as eluent. Recrystallization of **3** from acetone afforded crystalline white prisms suitable for single-crystal X-ray diffraction analysis. M.P. 129 °C. FTIR (KBr): ν = 3072, 2942, 1741 (C=O), 1608, 1587, 1213, 1153, 1126, 1066, 1029 (C–O) cm^{-1}. ^{1}H-NMR (400 MHz, $CDCl_3$): δ = 7.21–7.27 (m, 1H), 7.31 (td, *J* = 1.1, 7.6 Hz, 1H), 7.50–7.56 (m, 2H), 7.60–7.64 (m, 1H), 7.66 (d, *J* = 8.0 Hz, 1H), 8.28 (td, *J* = 1.8, 7.6 Hz, 1H), 8.59 (dd, *J* = 1.6, 8.8 Hz, 1H), 8.94 (dd, *J* = 1.6, 4.2 Hz, 1H) ppm. ^{13}C-NMR (100 MHz, $CDCl_3$): δ = 117.3 (CH, d, $J_{C\text{-}F}$ = 22.0 Hz), 117.9 (C, d, $J_{C\text{-}F}$ = 9.5 Hz), 121.6 (CH), 122.6 (CH), 124.3 (CH, d, $J_{C\text{-}F}$ = 4.4 Hz), 126.2 (CH), 127.5 (C), 129.1 (C), 133.1 (CH), 133.2 (CH), 135.4 (CH, d, $J_{C\text{-}F}$ = 8.8 Hz), 141.8 (C), 146.6 (C), 151.2 (CH), 162.7 (C, d, $J_{C\text{-}F}$ = 261.8 Hz), 162.8 (C, d, $J_{C\text{-}F}$ = 3.6 Hz) ppm. MS (EI, 70 eV) *m*/*z* (%): 303/301 (3/9) [M^+], 123 (100), 95 (21), 75 (8). HRMS (ESI+): calcd. for $C_{16}H_{10}ClFNO_2^+$ 302.0384 [M+H]$^+$; found: 302.0378.

Crystal Data: $C_{16}H_9ClFNO_2$ (M = 301.69 g/mol): monoclinic, space group *P* 2_1/c (No. 14), *a* = 7.5003(6) Å, *b* = 22.0264(16) Å, *c* = 8.5046(7) Å, α = 90.0, β = 105.547(7), γ = 90.0, V = 1353.59(19) $Å^3$, Z = 4, T = 293(2) K, μ(MoKα) = 0.297 mm^{-1}, Dcalc = 1.480 Mg/m^3, 14033 reflections measured (3.372° ≤ θ ≤ 27.664°), 3079 unique (Rint = 0.0274, Rsigma = 0.0181) which were used in all calculations. The final R1 was 0.0524 (I > 2_(I)) and wR2 was 0.0635 (all data).

Data Collection and Refinement Details: Diffraction data were collected on a Rigaku XTABLAB P-200 DS diffractometer using CrystalClear [21]; using graphite monochromated MoK$_\alpha$ radiation (0.71073 Å). The corrected data were solved by direct methods with *SHELXS-2014* [22] and refined by full-matrix methods on F^2 with *SHELXL-2014* [23]. All H-atoms, were positioned at geometrically idealized positions, C—H= 0.9300 Å, and were refined using a riding model approximation with Uiso(H) = 1.2 Ueq(parent atom). Correctness of the model was confirmed by low residual peaks (0.418) and holes (-0.342 e.Å^3) in the final difference map. (CCDC 1522239 contains the supplementary crystallographic data for this paper. These data can be obtained free of charge via http://www.ccdc.cam.ac.uk/conts/retrieving.html (or from the CCDC, 12 Union Road, Cambridge CB2 1EZ, UK; Fax: +44 1223 336033; E-mail: deposit@ccdc.cam.ac.uk).

Supplementary Materials: Copies of the ^{1}H-, ^{13}C-NMR, DEPT-135 and Mass spectra, and the checkCIF and CIF files for compound **3**, can be found online.

Acknowledgments: Authors thank Universidad del Valle for financial support – Project number CI-71073. JCC and JP thank Universidad de Los Andes and JAH also thanks Universidad Industrial de Santander (UIS), for partial financial support.

Author Contributions: J.C.C. designed and performed the experiments; J.C.C., R.A and J.P. analyzed the IR, MS and NMR spectral data; R.M-F. and J.C.C. wrote the manuscript. R.M-F. and J.A.H. performed the measurement and analysis of the X-ray experiments. All authors read and approved the final manuscript.

Conflicts of Interest: The authors declare no conflict of interest.

References and Notes

1. Klingenstein, R.; Melnyk, P.; Leliveld, S.R.; Ryckebusch, A.; Korth, C. Similar structure-activity relationships of quinoline derivatives for antiprion and antimalarial effects. *J. Med. Chem.* **2006**, *49*, 5300–5308. [CrossRef] [PubMed]
2. Das, P.; Deng, X.; Zhang, L.; Roth, M.G.; Fontoura, B.M.A.; Phillips, M.A.; De Brabander, J.K. SAR-based optimization of a 4-quinoline carboxylic acid analogue with potent antiviral activity. *ACS Med. Chem. Lett.* **2013**, *4*, 571–521. [CrossRef] [PubMed]
3. Sabatini, S.; Gosetto, F.; Manfroni, G.; Tabarrini, O.; Kaatz, G.W.; Patel, D.; Cecchetti, V. Evolution from a natural nucleus to obtain 2-(4-propoxyphenyl)quinoline derivatives as potent inhibitors of the *S. aureus* NorA efflux pump. *J. Med. Chem.* **2011**, *54*, 5722–5736. [PubMed]
4. Chioua, M.; Sucunza, D.; Soriano, E.; Hadjipavlou-Litina, D.; Alcázar, A.; Ayuso, I.; Oset-Gasque, M.J.; González, M.P.; Monjas, L.; Rodríguez-Franco, M.I.; et al. α-Aryl-*N*-alkyl nitrones, as potential agents for stroke treatment: Synthesis, theoretical calculations, antioxidant, anti-inflammatory, neuroprotective, and brain-blood barrier permeability properties. *J. Med. Chem.* **2012**, *55*, 153–168. [CrossRef] [PubMed]
5. Hammarström, L.G.J.; Harmel, R.K.; Granath, M.; Ringom, R.; Gravenfors, Y.; Färnegardh, K.; Svensson, P.H.; Wennman, D.; Lundin, G.; Roddis, Y.; et al. The oncolytic efficacy and in vivo pharmacokinetics of [2-(4-chlorophenyl)quinolin-4-yl](piperidine-2-yl)methanol (vacquinol-1) are governed by distinct stereochemical features. *J. Med. Chem.* **2016**, *59*, 8577–8592. [CrossRef] [PubMed]
6. Degorce, S.L.; Barlaam, B.; Cadogan, E.; Dishington, A.; Ducray, R.; Glossop, S.C.; Hassall, L.A.; Lau, A.; McGuire, T.M.; Nowak, T.; et al. Discovery of novel 3-quinoline carboxamides as potent, selective, and orally bioavailable inhibitors of ataxia telangiectasia mutated (ATM) kinase. *J. Med. Chem.* **2016**, *59*, 6281–6292. [CrossRef] [PubMed]
7. Tardito, S.; Barilli, A.; Bassanetti, I.; Tegoni, M.; Bussolati, O.; Franchi-Gazzola, R.; Mucchino, C.; Marchiò, L. Copper-dependent cytotoxicity of 8-hydroxyquinoline derivatives correlates with their hydrophobicity and does not require caspase activation. *J. Med. Chem.* **2012**, *55*, 10448–10459. [CrossRef] [PubMed]
8. For a review, see Andersson, M.I.; MacGowan, A.P. *J. Antimicrob. Chemother.* **2003**, *51* (Suppl. S1), 1–11. [PubMed]
9. Rabbani, M.G.; Islam, Md.R.; Ahmad, M.; Hossion, A.M.L. Synthesis of some NH-derivatives of ciprofloxacin as antibacterial and antifungal agents. *Bangladesh J. Pharmacol.* **2011**, *6*, 8–13. [CrossRef]

10. Adsule, S.; Barve, V.; Chen, D.; Ahmed, F.; Dou, Q.P.; Padhye, S.; Sarkar, F.H. Novel Schiff base copper complexes of quinoline 2-carboxaldehyde as proteasome inhibitors in human prostate cancer cells. *J. Med. Chem.* **2006**, *49*, 7242–7246. [CrossRef] [PubMed]
11. Moreno-Fuquen, R.; Mosquera, F.; Kennedy, A.R. 2,4,6-Trinitrophenyl furan-2-carboxylate. *Acta Cryst.* **2013**, *E69*, o1682. [CrossRef] [PubMed]
12. Moreno-Fuquen, R.; Hernández, G.; Ellena, J.; De Simone, C.; Tenorio, J.C. 5-Chloroquinolin-8-yl furan-2-carboxylate. *Acta Cryst.* **2013**, *E69*, o501. [CrossRef] [PubMed]
13. Moreno-Fuquen, R.; Hernández, G.; Kennedy, A.R. 4-Formyl-2-nitrophenyl benzoate. *Acta Cryst.* **2014**, *E70*, o268. [CrossRef] [PubMed]
14. Moreno-Fuquen, R.; Mosquera, F.; Ellena, J.; Tenorio, J.C. 2,4,6-Trinitrophenyl 3-bromobenzoate. *Acta Cryst.* **2014**, *E70*, o689. [CrossRef] [PubMed]
15. Moreno-Fuquen, R.; Hernández, G.; Ellena, J.; De Simone, C.; Tenorio, J.C. Crystal structure of 4-formyl-2-nitrophenyl-4-chloro-2-nitrobenzoate. *Acta Cryst.* **2015**, *E71*, o940. [CrossRef] [PubMed]
16. This compound is supplied by MCULE, among others: https://mcule.com/mcule-5727823188/ under the CAS Number 5727823188.
17. Mukherjee, A.; Tothadi, S.; Desiraju, G.R. Halogen bonds in crystal engineering: Like hydrogen bonds yet different. *Acc. Chem. Res.* **2014**, *47*, 2514–2524. [CrossRef] [PubMed]
18. Wang, H.; Wang, W.; Jin, W.J. σ-Hole bond vs π-hole bond: A comparison based on halogen bond. *Chem. Rev.* [CrossRef] [PubMed]
19. Lei, G. 8-Quinolyl benzoate. *Acta Cryst.* **2006**, *E62*, o4666–o4667. [CrossRef]
20. Desiraju, G.R.; Parthasarathy, R. The nature of halogen ... halogen interactions- Are short halogen contacts due to specific attractive forces or due close packing of nonspherical atoms. *J. Am. Chem. Soc.* **1989**, *111*, 8725–8726. [CrossRef]
21. Rigaku. *CrystalClear*; Rigaku Corporation: Tokyo, Japan, 2008.
22. Sheldrick, G.M. A short history of SHELX. *Acta Cryst.* **2008**, *A64*, 112–122. [CrossRef] [PubMed]
23. Sheldrick, G.M. Crystal structure refinement with SHELXL. *Acta Cryst.* **2015**, *C71*, 3–8.